

# Trailing-Edge Region of Airfoils

B. E. Thompson\*

*Scientific Research Associates, Inc., Glastonbury, Connecticut*  
and

J. H. Whitelaw†

*Imperial College of Science and Technology, London, England, United Kingdom*

Measured and calculated results obtained in a set of trailing-edge flows are examined to consolidate understanding of the requirements and implications for airfoil calculation methods. The experiments investigated sharp, round, and blunt trailing edges, attached and separated turbulent boundary layers, and boundary-layer interaction with the wake of an airfoil on the suction side. Emphasis is placed on higher angles of attack and on the consequences of flow separation. A combination of inviscid-flow calculations, interactive boundary-layer calculations with equations in integral and differential form, and Reynolds-averaged Navier-Stokes calculations have been used to confirm conclusions based on these experiments and to assess implications for approximations. The measurements suggest, and calculations confirm, that streamwise and normal momentum equations need to be solved in calculations of trailing-edge flows and that, in particular, normal pressure gradients and turbulence normal stresses need to be represented. Turbulence production from Reynolds normal stresses can exceed turbulence shear stress production in a separated flow, and this has implications for turbulence models. The ability to calculate contributions to lift and drag is considered within the trailing-edge region, and the experimental and computational uncertainties incurred in the results are examined.

## Nomenclature

$C, c$	= chord length
$C_d$	= drag coefficient
$C_m$	= moment coefficient
$C_p$	= pressure coefficient $(P - P_{\text{REF}})/\frac{1}{2}\rho U_{\text{REF}}^2$
$i, j$	= subscripts for streamwise and normal coordinate directions
$k$	= turbulence kinetic energy
$P$	= pressure
$P_{\text{REF}}$	= static pressure at boundary-layer trip
$s, n$	= boundary-layer coordinates (see Fig. 1)
$t$	= time
$U$	= streamwise velocity ( $x_1$ -direction)
$U_{\text{REF}}$	= freestream velocity above boundary-layer trip
$V$	= normal velocity ( $x_2$ -direction)
$x, y$	= wake coordinates (see Fig. 1)
$z$	= spanwise direction
$\alpha$	= angle of incidence
$\delta$	= boundary-layer thickness ( $U/U_e$ of 0.98)
$\epsilon$	= rate of dissipation of turbulent kinetic energy
$\rho$	= density
$\mu$	= kinematic viscosity
$\nu$	= dynamic viscosity ( $\mu/\rho$ )
$'$	= superscript denotes fluctuating component
$\langle \rangle$	= time-averaged quantity

## I. Introduction

THE development of calculation methods for the properties of the flow around airfoils and wings has received considerable attention in recent years.<sup>1,2</sup> Solutions of inviscid-flow equations provide useful information of lift, and interac-

tion of these solutions with different forms of the viscous-flow equations has allowed consideration of near-wall properties, including overall drag.<sup>3</sup> Advances in computer technology have led to growth of expectations to include the possibility of calculations of the flow around complete air frames, but quantification of accuracy remains difficult to establish.

The problem of establishing accuracy is present in the airfoil flows considered here and can be discussed from the standpoints of requirements and limitations. It has been possible to calculate lift of a simple airfoil at low angle of attack within about 10% for many years. The current requirement is to calculate values considerably better than this and for angles of attack up to those approaching stall. Drag is a second requirement, and it would be advantageous to be determined with an accuracy approaching a few percent. Reduced accuracy may be acceptable for landing, maneuvering, and takeoff configurations since they represent a small portion of the total flight cycle. Since results are presented frequently in terms of pressure coefficients with local regions of steep gradient, it can be difficult to assess the accuracy of a lift calculation and graphs of lift coefficient against drag coefficient can obscure calculation errors.

The limitations of a calculation originate in numerical and physical assumptions. The numerical errors are usually greatest with the least approximate physical assumptions, as in the solution of the time-dependent Navier-Stokes equations, and may be a consequence of limitations in the solution procedure or practical constraints associated with computers and expense. Numerical errors also occur in the solution of inviscid equations and integral or differential forms of the boundary-layer equations, but they can often be arranged to be small. Physical assumptions are involved in any reduced form of transport equations and, to achieve accuracies of the order of those indicated above, require representation of turbulent aspects of the flow either explicitly in turbulence models or implicitly in velocity-profile assumptions.

In calculations that involve reduced forms of the Navier-Stokes equations, turbulence assumptions, boundary conditions, and a numerical solution procedure, the accuracy of numerical assumptions can seldom be determined directly, and measurements provide the essential basis for the evaluation of uncertainty. It is important, therefore, to examine the

Received Feb. 7, 1988; revision received Aug. 25, 1988. Copyright © 1988 by B. E. Thompson. Published by the American Institute of Aeronautics and Astronautics, Inc., with permission. All rights reserved.

\*Research Scientist. Member AIAA.

†Professor, Fluids Sections, Department of Mechanical Engineering.

available experiments to determine the requirements that they reveal, and then to assess the implications for calculation methods. This paper does this in relation to trailing-edge flows that comprise one limited, but identifiable, region of an airfoil flow. Thus, questions associated with the leading edge, regions of strong favorable pressure gradient, and transition are omitted here to allow concentration on the region of the airfoil close to its trailing edge and of the wakes. The present emphasis is on the higher angles of attack associated with high lift and the consequences of suction-surface flow separation.

The following section considers the implications of the series of experiments reported by Thompson and Whitelaw,<sup>4-7</sup> Thompson,<sup>8</sup> Adair et al.,<sup>9,10</sup> Reis,<sup>11</sup> Adair,<sup>12</sup> and Acharya et al.,<sup>13</sup> which involve configurations of a trailing plate at deflection angles of 14, 16, and 17.5 deg and detailed measurements, of velocity and pressure characteristics in the vicinity of the trailing edge. The flows over those configurations emphasize the trailing-edge region, but differ from airfoil flows in that the wake has some features more closely related to those of a plane mixing region. To make the link with airfoil flows, the more important conclusions are considered in relation to the airfoil flows of Nakayama.<sup>14,15</sup> Each of these flows has been investigated with specific objectives for that configuration, but there is an overall interrelationship between these flows that provides further understanding useful to the development of models and calculation methods and to the designer, that needs to be presented, and is the subject of this paper.

The third section of the paper examines the equations of motion and the various reduced forms used in calculation methods. The discussion places emphasis on the requirements indicated by the measurements examined in the following section and the likely consequences of their omission. The fourth section considers some calculated results obtained with different equation forms and relates the findings to those of the previous two sections. The paper ends with a summary of the more important conclusions.

## II. Physical Information

The series of experimental investigations carried out at Imperial College led to results that included distributions of static pressure, two components of mean velocity, Reynolds normal and shear stresses, and some spectral information. Two aspects of the results are highlighted in the following paragraphs and correspond to the variations of mean pressure and of turbulence normal stresses. The first has consequences for the choice of the form of the viscous-flow equations and the second for the choice of turbulence model within time-averaged equations. Before discussing implications of the results, it is necessary to assess the experimental configuration, the two-dimensionality of the mean flow and the nature of the wake, and to establish that they are representative of airfoil flows.

The experimental arrangement is shown in Fig. 1 and offers the advantage of concentration on the near trailing-edge region and the disadvantages associated with the use of a comparatively small wind tunnel, including deviations from two-dimensionality and different freestream velocities on the two sides of the trailing edge. These two disadvantages require further comment since they imply differences from airfoil flows. Thus, although later comparisons with the airfoil results of Nakayama confirm the present conclusions, it is useful to examine the implications of deviations from two-dimensionality and a normal wake before examining pressure and normal-stress distributions.

The deviations from two-dimensionality are associated with the growth of the secondary flows in the corners formed by the model and the side walls of the wind tunnel and increased with deflection angle. Passive splitter plates were attached to the side walls of the wind tunnel to break up the secondary flows, and resulted in a region of two-dimensional mean flow over a limited span of the tunnel. Spanwise distributions of mean values of pressure, velocity, and Reynolds stresses were found

to be constant over a minimum of 40% of the tunnel span, and the two-dimensional integral momentum equations balanced within about 6% of the largest local term, which is within experimental uncertainty. Figure 2 shows examples of the region of constant surface static pressure at 90% of chord in the attached boundary layers and separated regions of Thompson and Whitelaw<sup>4</sup> and Reis.<sup>11</sup> The flow of Reis<sup>11</sup> involving a boundary layer interacting with the wake of an upstream airfoil has the largest momentum deficit of those considered here and, although it is the most susceptible to three-dimensional effects, mean velocity distributions in the wake at locations on and off the centerline (Fig. 2b) reveal only small deviations.

The wakes that resulted from the present arrangements are peculiar to this type of flow configuration. The difference in the freestream total pressures on the upper and lower side of the plate results in a turbulence structure, although not mean flow patterns, which is proportioned differently from that usually associated with symmetric and asymmetric airfoil wakes. Reynolds stress distributions are similar but magnitudes are different so that, for example, there is only one peak in the cross-stream distribution of longitudinal normal stress.

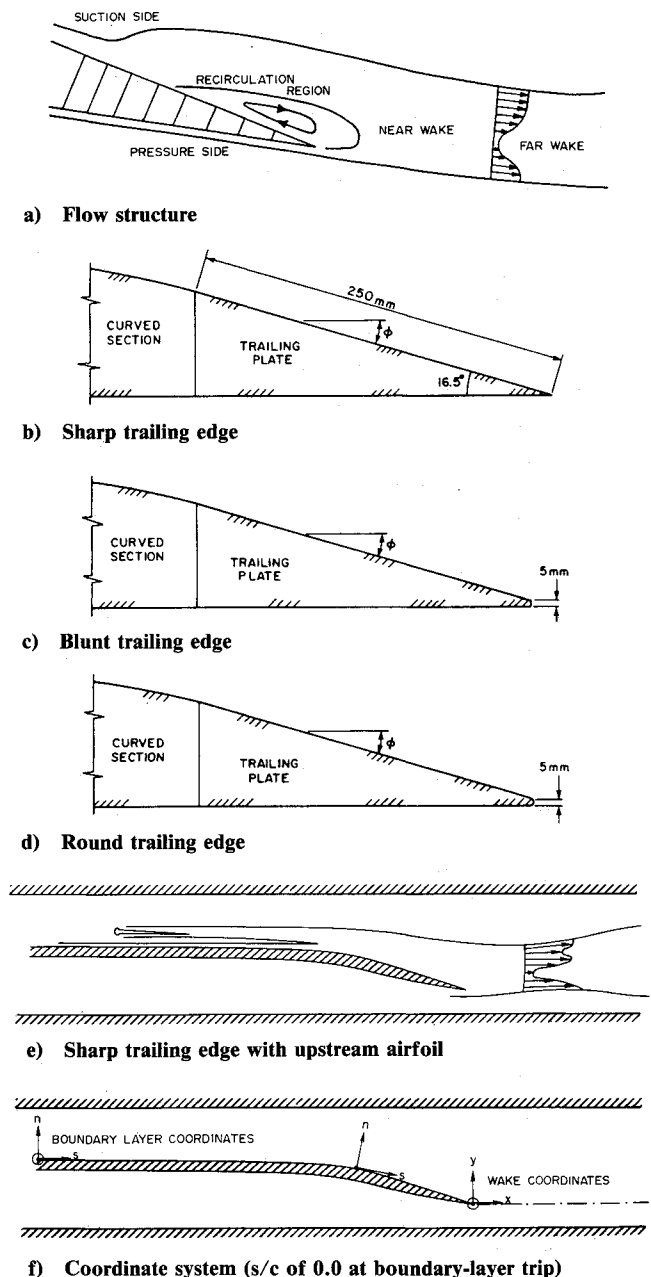


Fig. 1 Trailing-edge configurations.

Also, the Reynolds stresses are larger in the pressure-side shear layer in airfoil wakes, whereas they are larger in the suction-side shear layer in the present flows. The far wake of the present arrangement develops into a plane mixing layer with associated turbulence production. The wake is wide so that the strain rate is small, and turbulence production is about the same magnitude as the other transport processes.

These comments on two-dimensionality and on the nature of the wake provide support for the further examination of the flow characteristics. The profiles of static pressure obtained with the three deflection angles are shown in Figs. 3 and 4 and were obtained with surface taps and a five-hole probe, respectively, on a coordinate system corresponding to orthogonals to the surface and, in the wake, normal to the tunnel roof. There are uncertainties associated with the use of the taps and the probe, and careful examination suggested that they might be as large as 0.0035 and 0.034 of  $C_p$ , respectively; they are not, however, sufficiently large to influence the following conclusions that are extracted from Figs. 3 and 4. The longitudinal adverse pressure gradient is shown in Fig. 3 to increase with deflection angle. Cross-stream pressure gradient also increases with the angle of deflection of the trailing plate and extends

over a larger portion of the flow, as shown in Fig. 4. Cross-stream pressure gradients in the vicinity of the trailing edge are apparently significant at small incidence (also see Nakayama<sup>15</sup>), and the present flows quantify the increase in magnitude and importance with greater asymmetry between suction and pressure-side boundary layers and, thus, with increase in angle of attack.

Terms in the equations that represent transport of stream-wise and normal momentum were obtained by substitution of measured ensemble-averaged quantities from hot-wire, flying-wire, and impact probes into discretized expressions for each term. These terms are shown in Fig. 5 and suggest that normal

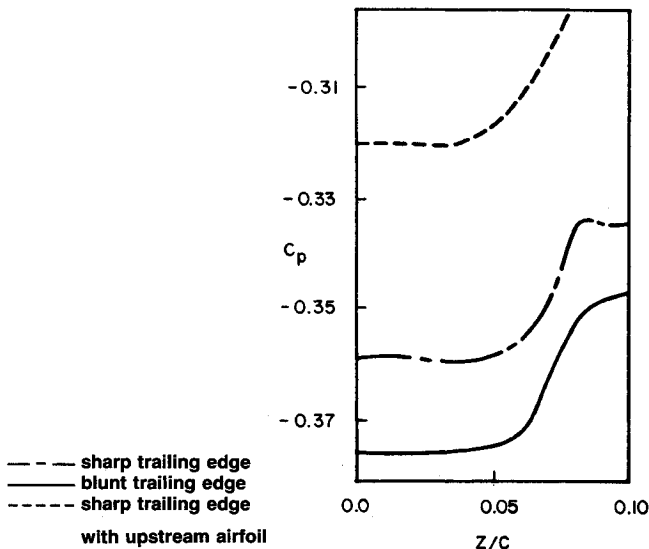


Fig. 2a Spanwise surface pressure distribution at 17.5-deg incidence and  $s/c$  of 0.9;  $z$  is the spanwise coordinate direction. Tunnel side wall is at  $z/c$  of 0.134.

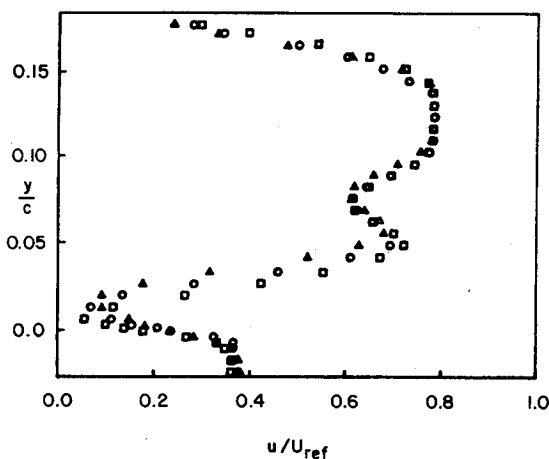


Fig. 2b Profiles of mean velocity at  $s/c$  of 1.066. Trailing-edge plate at 17.5-deg incidence with upstream airfoil,  $z/c$  of 0.0  $\square$ ; 0.04  $\circ$ ; 0.75  $\Delta$ . Tunnel side wall at  $z/c$  of 0.134.

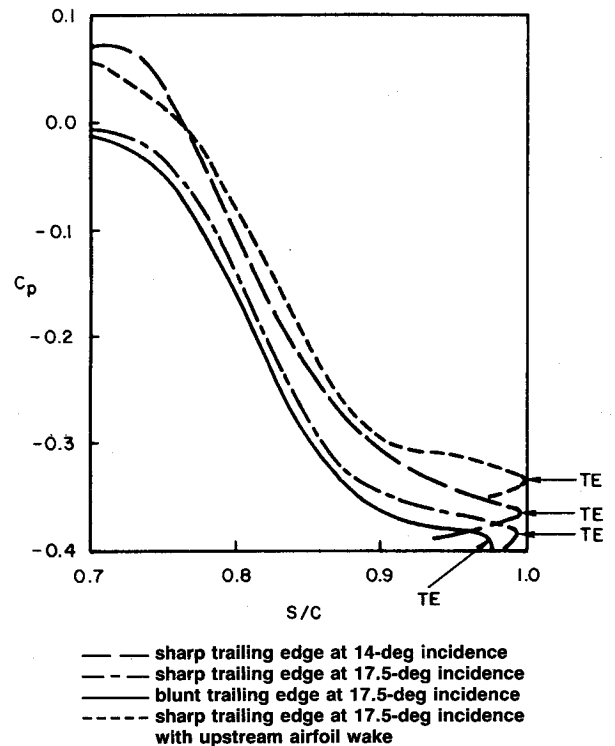


Fig. 3 Surface pressure distribution. TE indicates trailing edge with upper and lower surface measurements above and below, respectively.

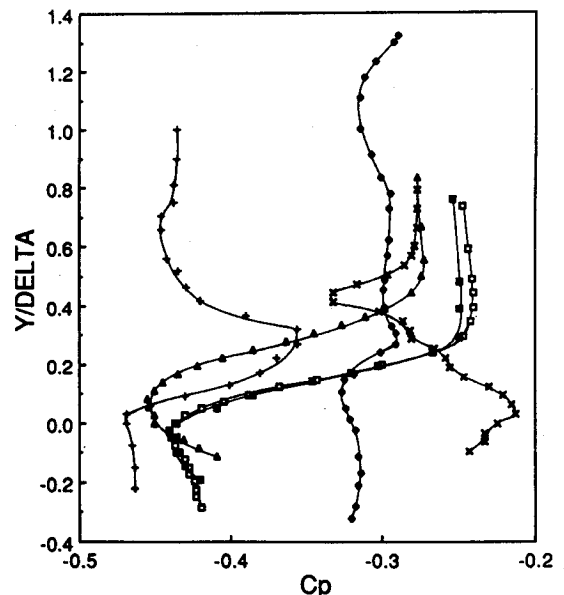
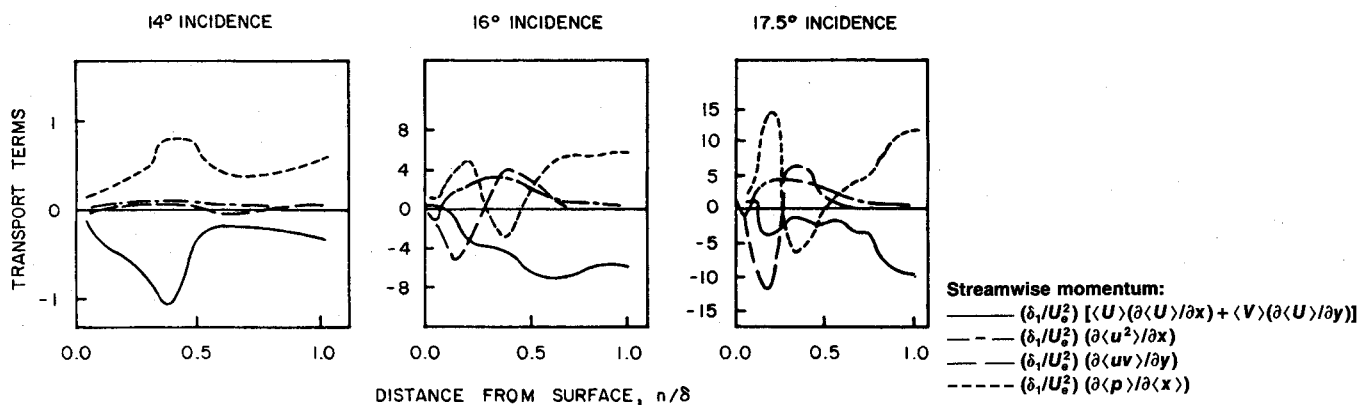
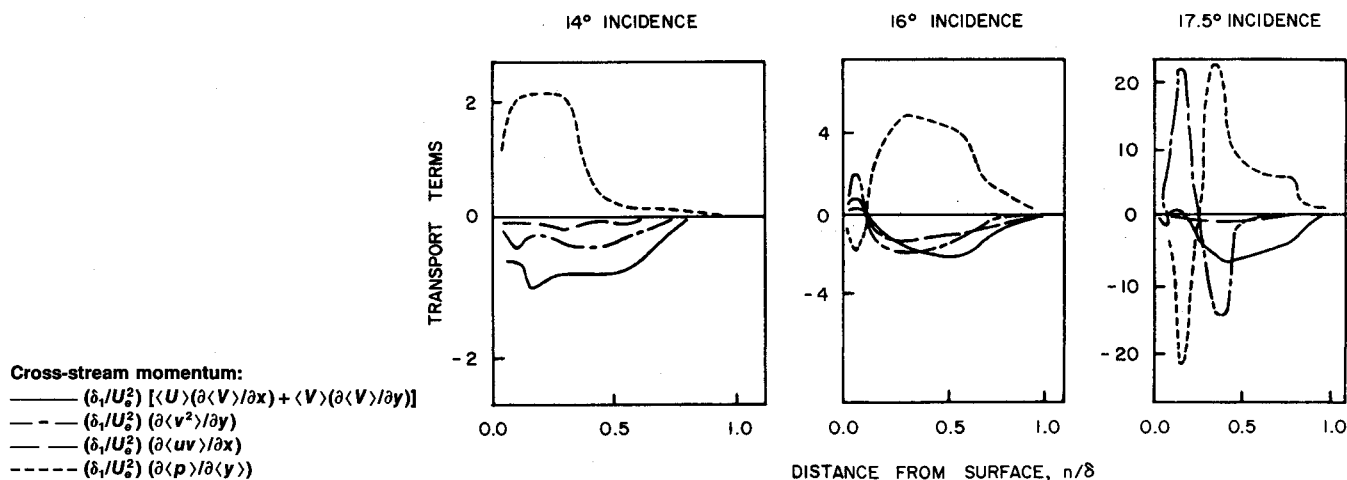


Fig. 4 Distribution of static pressure at  $x/c$  of 0.13 in the wake.



a) Streamwise momentum equation



b) Cross-stream momentum equation

Fig. 5 Distributions of terms in momentum transport equations at  $s/c$  of 0.9.

pressure gradients are important. In order to verify this conclusion and to discount any misinterpretation associated with experimental uncertainty, values of cross-stream pressure gradient obtained from measurements were compared with those obtained from imbalance in the cross-stream momentum transport equation and were found to agree within 15%.

The relative importance of the cross-stream pressure gradient and the need to solve the normal momentum equation in calculation methods are apparent in the flow characteristics measured with angles of attack that approach or result in boundary-layer separation. With the trailing plate at 14-deg incidence and the suction-side boundary layer close to separation, streamwise and normal pressure gradients were of the same magnitude, and were greater than transport terms associated with turbulence quantities, except in the near wake where turbulence transport increased, and all of the terms were of similar magnitude. The pressure gradients were associated with mean flow curvature, which was apparent from upstream of the trailing edge into the curved wake.

With trailing-edge separation and deflection angles of 16 and 17.5 deg, the cross-stream pressure gradient was larger than the streamwise pressure gradient in the separated flow region near the trailing edge. Cross-stream pressure gradients were measured to be larger than in the attached flow with the 14-deg deflection angle; cross-stream pressure gradients were up to three times larger with the 16-deg deflection angle, and the separation occurred 6% of the chord upstream of separation, and up to 10 times larger with 17.5-deg incidence and separation located 13% upstream of the trailing edge. Flow curvature and turbulence effects were found to be large in the shear layer that separated forward and back flow, and this

resulted in pressure gradients in both streamwise and cross-stream directions around the periphery of the back-flow region. In the back-flow region, cross-stream and streamwise velocity components were similar with values less than 10% of the freestream velocity so that convection is small compared to that in attached boundary layers, and pressure gradients balance turbulence transport effects. The cross-stream pressure gradient increases with the streamwise and cross-stream dimensions of the recirculating flow region and is required to represent physical behavior observed in the vicinity of the recirculation region.

Pressure gradients also affect development of the wake. Favorable streamwise gradients accelerate the near-wake flow with attached boundary layers at the trailing edge and, similarly, there is a mild favorable pressure gradient in the vicinity of the downstream stagnation point of the recirculation region. The corresponding cross-stream pressure gradient acts to decrease the width of the wake, so that the minimum width is just downstream of the trailing edge or downstream of the stagnation point and plays an important role in determining the curved trajectory of the wake. Flow curvature in the wake depends in part on the local momentum deficit and, thus, on angle of attack in that, for example, the wake of a separated flow with its larger momentum deficit is more easily deflected, and thus more likely to be highly curved, than the wake of attached boundary layers in which inertial effects are more predominant. The geometry of the trailing edge also affects the wake flow. In the case where the trailing plate was inclined at 14-deg incidence and the boundary layer remained attached, the effect of the geometry of the trailing edge was confined to a small region in the near wake whose cross-stream and down-

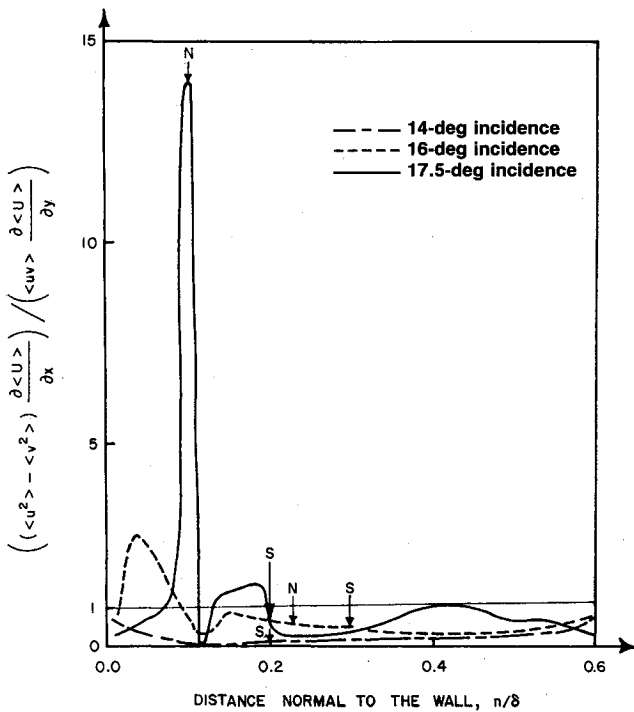


Fig. 6 Ratio of magnitude of normal-stress and shear-stress production of turbulence kinetic energy at the trailing edge. *N* and *S* mark maxima of normal and shear stress production, respectively.

stream dimensions were 10% and 55%, respectively, of the boundary-layer thickness at the trailing edge. The wake flow in this case was important mainly in the determination of base pressure. In contrast, with the trailing plate at 17.5-deg incidence that resulted in boundary-layer separation, the structure of the separated and wake flow regions was significantly affected by the trailing-edge geometry. For example, the location of mean flow streamline detachment as measured with the flying-wire, which was 12.3% of chord upstream of the sharp trailing edge of 0.0033 chord thickness. The distributions of surface pressure and mean velocity were significantly altered,<sup>5</sup> which indicates that both lift and drag are affected. The results suggest that accurate calculation of lift, drag, and the onset of separation on airfoils as a function of incidence requires representation of the effects of trailing-edge shape and thickness on the pressure gradients in the direction across the boundary layer and in the streamwise direction, especially in the wake.

Comparisons with the flows of Nakayama<sup>14,15</sup> around airfoils at 4- and 12-deg incidence show many similarities, and also suggest that variations in normal momentum need to be represented in calculations of the flow at 14-deg incidence, and that of Nakayama<sup>14</sup> at 4 deg shows that the streamwise and normal pressure gradients are distributed in a similar manner with the pressure-side boundary layer less important to the wake development. One difference is the total pressure deficit on the pressure side of the plate at 14-deg incidence which, although it does not affect the mean flow patterns significantly, changes the turbulence structure because of decreased turbulence production in the wake, as discussed previously, and presents a difficulty to calculation schemes that rely on equal values of total pressure in the freestream above and below the airfoil.

The flow at 16-deg incidence and that of Nakayama<sup>15</sup> with an airfoil at 12-deg incidence also show similarities, although experimental methods are different: Adair<sup>12</sup> used the flying-hot-wire anemometer of Thompson and Whitelaw,<sup>6</sup> whereas Nakayama<sup>15</sup> used laser-Doppler anemometry. Also, the flow configurations have different three-dimensional effects. Nevertheless, both experiments show large normal pressure

gradients and almost constant surface pressure near the trailing edge. The magnitude and distributions of flow curvature and its stabilizing and destabilizing effects on turbulence are similar.

The previous paragraphs deal with one aspect of the mean flow, and the discussion is now changed to consider the relative importance of turbulence normal-stress and shear-stress production. Measured values of mean and turbulence quantities were used to obtain the ratio of turbulence production by normal and shear stresses shown in Fig. 6. It is evident that normal-stress production is more important than shear-stress production in the vicinity of back flow. The effect, and corresponding need to represent normal-stress production, increases with increase in angle-of-attack. For calculation methods, this suggests that normal-stress production may be ignored for attached flows and possibly small regions of recirculation, but requires representation as the angle of attack approaches maximum lift. For moderate and large regions of back flow, the maximum values of normal-stress production along lines normal to the surface exceed the corresponding maximum shear-stress production in the vicinity of detachment or the downstream stagnation point, although at different locations across the profile. Normal-stress production achieves a maximum in the back flow close to the wall, whereas maxima of shear-stress production are associated with maxima in strain rate. This suggests that turbulence models based on eddy-viscosity assumptions will fail at large angles of attack because of their inability to represent normal-stress production in the back flow. The calculations of Thompson<sup>8</sup> with the  $k-\epsilon$  turbulence model tend to support this, and an additional, empirically based term was developed to represent the normal-stress contribution to production of turbulence kinetic energy in the near-wall recirculating region.

### III. Transport Equations

The time-dependent Navier-Stokes equations are assumed to be appropriate to the flows over airframes and may be expressed, together with mass conservation, in the incompressible form

$$\frac{\partial \bar{U}_i}{\partial x_j} = 0 \quad (1)$$

$$\frac{\partial \bar{U}_i}{\partial t} + \bar{U}_j \frac{\partial \bar{U}_i}{\partial x_j} = -\frac{1}{\rho} \frac{\partial \bar{P}}{\partial x_i} + \frac{1}{\rho} \frac{\partial}{\partial x_j} \left( \mu \frac{\partial \bar{U}_i}{\partial x_j} \right) \quad (2)$$

where  $\bar{\phantom{x}}$  indicates instantaneous quantities, and the subscript  $j$  is summed from Eqs. (1-3). Because this set of equations cannot be solved in sufficient detail to represent all turbulent scales, recourse is made to simpler forms. Reduced forms considered here include the two-dimensional, steady-flow equations, which may be expressed as

$$\frac{\partial \langle U \rangle}{\partial x} + \frac{\partial \langle V \rangle}{\partial y} = 0 \quad (3)$$

for continuity,

$$\langle U \rangle \frac{\partial \langle U \rangle}{\partial x} + \langle V \rangle \frac{\partial \langle U \rangle}{\partial y} = -\frac{1}{\langle \rho \rangle} \frac{\partial \langle P \rangle}{\partial x} \quad (4a)$$

$$\langle U \rangle \frac{\partial \langle V \rangle}{\partial x} + \langle V \rangle \frac{\partial \langle V \rangle}{\partial y} = -\frac{1}{\langle \rho \rangle} \frac{\partial \langle P \rangle}{\partial y} \quad (4b)$$

for inviscid flows, and

$$\begin{aligned} \langle U \rangle \frac{\partial \langle U \rangle}{\partial x} + \langle V \rangle \frac{\partial \langle U \rangle}{\partial y} = & -\frac{1}{\langle \rho \rangle} \frac{\partial \langle P \rangle}{\partial x} \\ & + \frac{1}{\langle \rho \rangle} \frac{\partial}{\partial y} \left( \mu \frac{\partial \langle U \rangle}{\partial y} \right) - \frac{\partial}{\partial y} \langle u'v' \rangle \end{aligned} \quad (5)$$

for viscous, boundary-layer flow. Equation (4) provides information about lift that can be improved by consideration of the viscous shear layer represented by Eq. (5), and the consequent interaction of the two equations provides information about drag. This approach has been taken by many authors including, for example, Seeborn and Newman,<sup>16</sup> Melnik et al.,<sup>17</sup> Gilmer and Bristow,<sup>18</sup> Williams,<sup>19</sup> Le Balleur,<sup>20</sup> Bradshaw et al.,<sup>21</sup> Veldman and Lindhout,<sup>22</sup> Cebeci et al.,<sup>23</sup> Van Dalsem and Steger,<sup>24</sup> and Adair et al.,<sup>10</sup> and discussed in the reviews by Briley and McDonald,<sup>25</sup> Cebeci et al.,<sup>26</sup> and Cebeci and Whitelaw,<sup>27</sup> for example. Other types of interaction involve the solution of thin shear-layer Navier-Stokes equations (see, e.g., Mehta et al.<sup>28</sup>) and the more general two-dimensional, time-averaged form of the Navier-Stokes equations:

$$\begin{aligned} \langle U \rangle \frac{\partial \langle U \rangle}{\partial x} + \langle V \rangle \frac{\partial \langle U \rangle}{\partial y} = & -\frac{1}{\langle \rho \rangle} \frac{\partial \langle P \rangle}{\partial x} \\ & + \langle \nu \rangle \left( \frac{\partial^2 \langle U \rangle}{\partial x^2} + \frac{\partial^2 \langle U \rangle}{\partial y^2} \right) \\ & - \frac{\partial}{\partial x} \langle u'^2 \rangle - \frac{\partial}{\partial y} \langle u'v' \rangle \end{aligned} \quad (6a)$$

$$\begin{aligned} \langle U \rangle \frac{\partial \langle V \rangle}{\partial x} + \langle V \rangle \frac{\partial \langle V \rangle}{\partial y} = & -\frac{1}{\langle \rho \rangle} \frac{\partial \langle P \rangle}{\partial y} \\ & + \langle \nu \rangle \left( \frac{\partial^2 \langle V \rangle}{\partial x^2} + \frac{\partial^2 \langle V \rangle}{\partial y^2} \right) \\ & - \frac{\partial}{\partial x} \langle v'^2 \rangle - \frac{\partial}{\partial y} \langle u'v' \rangle \end{aligned} \quad (6b)$$

In this latter case, a solution may be obtained by generating a finite-difference mesh, for example, with the inviscid flow equations and solving the complete time-averaged Navier-Stokes equations on the grid as, for example, by Thompson,<sup>8</sup> Briley et al.,<sup>29</sup> and Briley and McDonald<sup>30</sup> or by relaxing in the viscous terms as by Briley and McDonald.<sup>31</sup>

A major conflict occurs since Eqs. (3-5) can usually be solved with good numerical accuracy, but may inadequately represent the flowfield, especially at higher angles of attack; Eqs. (3) and (6) may represent the flowfield more accurately, but their solution can introduce numerical errors that are difficult to quantify. In both cases, the time-averaged nature of the equations implies that information has been disregarded, and an accurate solution to the equations may not be an accurate representation of the flow. The choice of a turbulence model to represent the Reynolds stress terms seeks to minimize this last difficulty, but cannot remove it.

The appraisal of the previous section has implications for the choice of equations. It is evident from Fig. 5 and the related discussions that the cross-stream pressure gradient can be of similar magnitude to, or larger than, the longitudinal pressure gradient, and that neither can be considered to be an order of magnitude less than that of the turbulence diffusion or convection terms. Further evidence for this is provided by the calculations of Thompson,<sup>8</sup> Reis,<sup>11</sup> and Reis and Thompson<sup>32</sup> obtained from the numerical solution of Eqs. (3) and (6) with hybrid combinations of bounded-skew-upwind differencing and upwind-control differencing and a modified version of the TEACH code as described by Thompson.<sup>8</sup> These solutions are subject to numerical uncertainty, but not to an extent which influences the conclusions that are drawn in the discussion of Fig. 5. Estimated values of numerical error were obtained for calculations of the flow around the trailing plate at 17.5-deg incidence with and without the wake of an upstream airfoil element on the suction side. The estimate of

numerical uncertainty is the imbalance in Eq. (6a) when the constituent transport terms, shown in Fig. 7, were calculated from the numerical solution and compared to those obtained from higher-order approximation as described by McGuirk et al.<sup>33</sup> The implication of imbalance terms in excess of 10% of the largest transport term, i.e., net convection, net diffusion, or net source terms in the local cell balances, is that numerical error makes a substantial contribution to diffusion so that profiles of the dependent variable spread at a greater rate than is represented by the differential transport equations: the finite-difference equations have significantly larger diffusion than the transport equations from which they were derived. Numerical errors were negligible over about 70% of the calculation domain in calculations both with and without the suction-side wake.

There are three regions where the imbalance term shown in Fig. 7 indicates numerical errors of the order of magnitude of local pressure gradient terms: in the potential flow, in the suction-side shear layer that borders forward and reversed flow, and in the vicinity of the trailing edge downstream of where the pressure-side boundary layer enters the calculation domain. In the potential flow, convection balances pressure gradient, and any numerical diffusion appears large relative to physical diffusion. In the shear layers that divide forward and reversed flow, the largest imbalance terms are found. The magnitude of the imbalance here is comparable to the physical diffusion in only this small but important region of the flow on the freestream side of both shear layers. Numerical errors were unimportant inside the separation bubble, as is evident by the differences between bounded-skew and hybrid upwind-

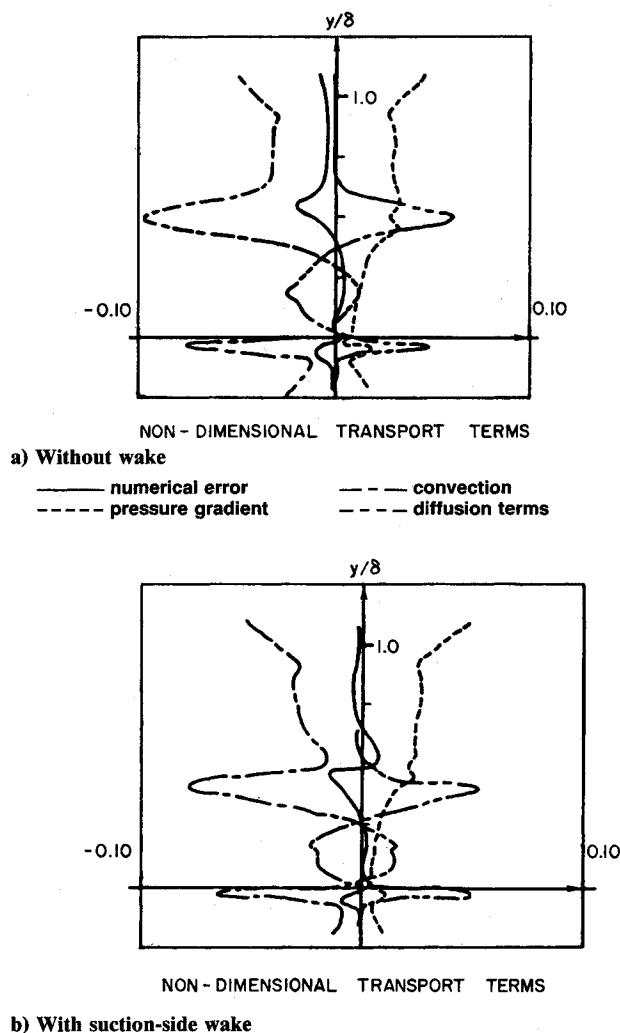


Fig. 7 Assessment of numerical error at  $x/c$  of 1.12 with 17.5-deg incidence. Terms are nonmimensionalized with  $\delta_1/U_\infty^2$ .

central difference calculation shown in Fig. 8; the bounded-skew scheme calculated slightly larger cell Peclet numbers as a consequence of less numerical diffusion in the outer shear layer and, therefore, employed central differences over 60% rather than 75% of the back flow as in the upwind-central calculations; however, differences in the calculated recirculating flow were insignificant.

Figure 8 shows the effect of different numerical approximations for convection terms and helps to quantify the corresponding numerical error. The profile of mean velocity and the streamwise variation of static pressure are not greatly affected by the different numerical representations of convection, and the discrepancies between measured and calculated results are not substantially improved. Results obtained with the bounded-skew scheme were in somewhat better general agreement with trends of the measurements and showed less numerical error,<sup>32</sup> but calculated values were not significantly improved, and both calculations were different from measurements. Turbulence quantities were calculated to be very similar in the bounded-skew and hybrid upwind-central calculations,<sup>32</sup> and this suggests that improvements in the turbulence model assumptions may be important to successful calculations of the influence of separation. The contribution of the flow in the vicinity of the trailing edge to lift coefficients was within 3 and 2% of experimental values when obtained with hybrid bounded-skew-central-upwind and hybrid central-upwind approximations, respectively. The wakes of both calculations were in poor agreement with measurements and indicate that the calculated drag coefficient was at least 20% different from that of the measurements. Turbulence-model assumptions are apparently more important to the prediction of drag coefficient than to the calculation of lift coefficient.

Both calculation schemes gave results that quantitatively disagree with measurements, and the distributions of pressure and velocity characteristics differed to a degree that would have influence in aircraft design. The pressure distribution in the vicinity of the recirculating flow differed from the measured pressure coefficient around the location of mean streamline detachment. The bounded-skew calculation overpredicts  $C_p$  in the attached boundary layer and underpredicts it in the separated flow, but because of cancellation errors, gives an overall lift coefficient that is closer to the measured value. The freestream flow calculated with the bounded-skew scheme is in about 2% better agreement with measurements in the separated region and the wake, but in about 1% poorer agreement in the attached flow region, and this is a direct consequence of reduced numerical error. Numerical errors are not solely responsible for discrepancies: wall function and turbulence model approximations make a contribution to the overall error. It is difficult to separate these errors, to determine their source and, thus, to guide improvements to numerical or turbulence model approximations.

The importance of  $\partial P/\partial y$  in a curved wake is to be expected and requires consideration of some form of second momentum equation. The question arises as to the extent to which sensible results can be obtained without consideration of the wake and of the normal pressure gradient, and this depends on the angle of attack. At small angles of attack, lift should be well calculated with approximate representation of  $\partial P/\partial y$  or wake curvature at least in part, because the region with cross-stream pressure gradient, and associated flow curvature, extends over a small region around the trailing edge. Drag is less well calculated because neglect of these pressure gradients does not allow adequate representation of the development of the boundary layers, which is important to skin friction and form drag. As the angle of attack increases, the large cross-stream region of strong interaction near the trailing edge becomes larger and stronger so that lift and, to a degree, drag values are calculated to be increasingly different from measurements. At angles of attack approaching separation and higher, the strength of the interaction appears to have a first-order influence on boundary-layer development. This is

consistent with calculations (e.g., interactive boundary-layer calculations) that do not account for the distribution of pressure in the vicinity of the trailing edge, being successful in the calculation of lift, but are unable to obtain drag reliability at any angle of attack.

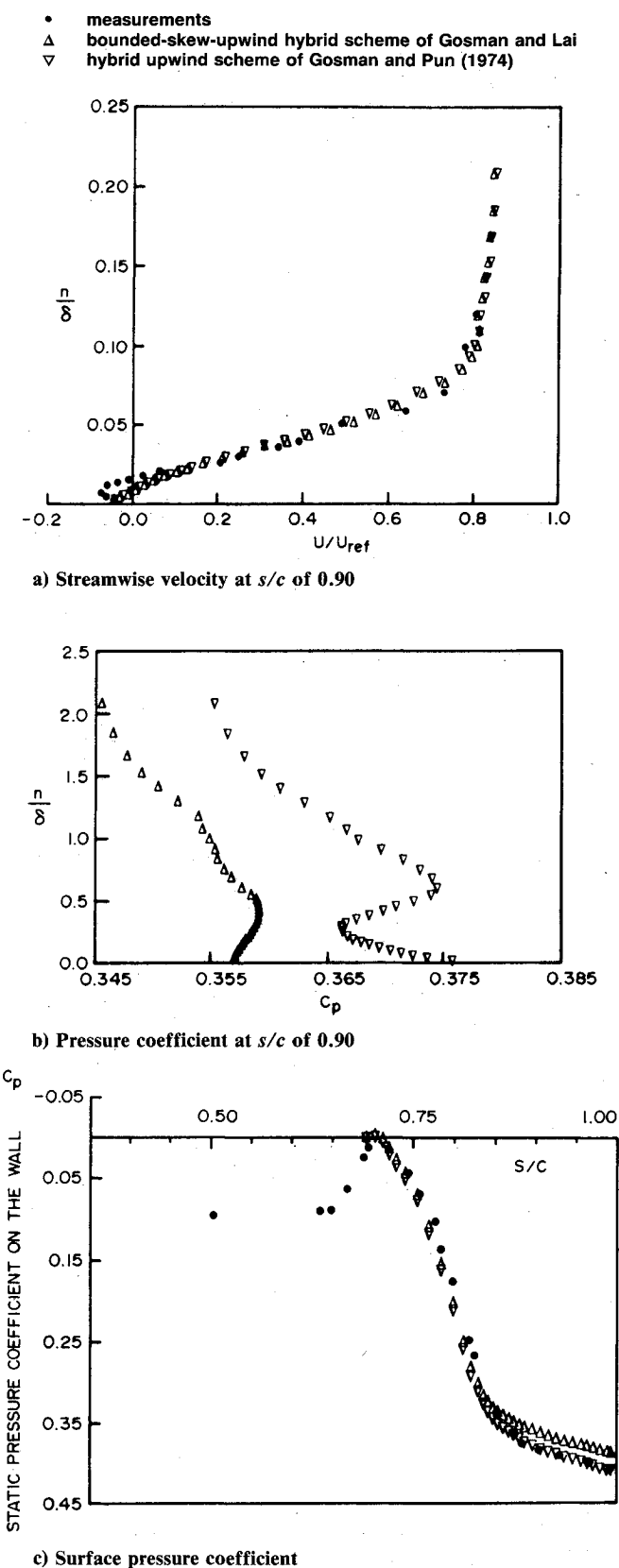


Fig. 8 Calculated results with trailing plate at 17.5-deg incidence.

#### IV. Calculated Results

The previous section emphasizes some of the implications of the experiments for calculation methods. In this section, the problem is reversed, and results are presented that have been obtained by interaction of Eqs. (3–5), including a second momentum equation in which normal pressure gradient is in balance with centrifugal acceleration, and by numerical solution of Eqs. (3) and (6). Again, the emphasis is on the trailing-edge region and on the higher angles of attack.

Cebeci et al.<sup>26</sup> and Briley and McDonald<sup>25</sup> refer to a number of calculations which demonstrate that interactive methods can be used to predict flows with small separation and are often preferred for practical applications, which include certain three-dimensional flows because their computational requirements are modest. The alternative approach is to solve the most complete form of the transport equations that is possible throughout the domain. Solutions of the time-averaged Navier-Stokes equations have been reviewed by Bradshaw et al.,<sup>34</sup> Shang,<sup>35</sup> Cebeci et al.,<sup>26</sup> MacCormack,<sup>36</sup> and Shang and Hanley<sup>37</sup> and applied to airfoils with separated and attached flows (see Shamroth and Gibeling,<sup>38</sup> Sugavanum and Wu,<sup>39</sup> Hegna,<sup>40</sup> Rhie and Chow,<sup>41</sup> and Adair et al.,<sup>9</sup> and three-dimensional aircraft configurations, for example by Shang and Scherr<sup>42</sup> and Chaderjian.<sup>43</sup> The results from these calculations show that the alternative provided by solution of the Navier-Stokes equations throughout the flow does not solve the problem in that numerical approximations, turbulence modeling assumptions, and boundary conditions introduce uncertainty. In principle, numerical errors can be eliminated with a combination of grid refinement and the use of higher-order finite-difference approximations such as those of Raithby<sup>44</sup> or Leonard,<sup>45</sup> but success has been limited because of computer capabilities and insufficient improvement offered by the higher-order methods (also see Leschziner<sup>46</sup>). It is also difficult to distinguish errors associated with turbulence models and numerical approximations, as discussed previously.

Several calculation procedures have been applied to separated flows. Gilmer and Bristow<sup>18</sup> solved with inviscid and viscous-corrected flow equations and obtained very good agreement with experimental values of lift and drag for single-element airfoils with separation, as shown in Fig. 9. An approximate representation of the separating streamline was arranged to give constant surface pressure downstream of separation. Poorer results were obtained for multielement

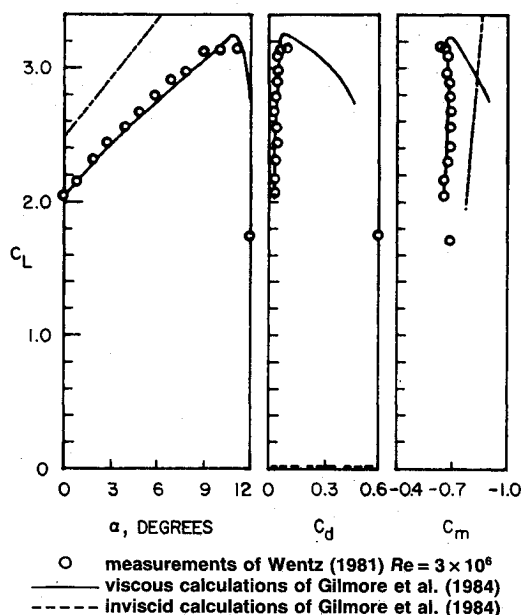


Fig. 9 Comparison of viscous and inviscid calculations of forces and moments on an airfoil with Fowler flap deflected 25-deg.

airfoils (see Gilmer et al.<sup>47</sup>), and this can be explained in part with the measurements of Reis<sup>11</sup> that show a significant effect on the structure of the recirculating flow and a larger variation in surface pressure downstream of separation than occurs without confluence of the suction-side boundary layer and wake of a second element.

The FLARE approximation has been used in calculations with recirculation because it allows solution by a forward-marching algorithm at reduced computational expense. It omits longitudinal convection and is likely to lead to errors, which increase with the size of the region of separated flow as discussed, for example, by Briley and McDonald.<sup>25</sup>

It seems unlikely that methods that integrate the flow in the viscous regions can be developed to predict flow over three-dimensional aircraft configurations, which include vortex, separated and confluent-boundary-layer flow regions. Integral methods rely on empirical information introduced through profile distribution assumptions and correlations (see Lock and Williams<sup>48</sup> and Williams,<sup>19</sup> for example), which restricts their application to the family of flows with which they were developed.

Second-order boundary-layer approximations such as those of East<sup>49</sup> are required in the vicinity of the trailing edge, and additional empirical information about the cross-stream pressure gradient and turbulence normal stresses need to be provided. The pressure distribution in the region of transition from boundary-layer to wake flow depends on parameters such as trailing-edge shape, confluence in the upstream boundary layers, separation and trailing-edge thickness, and development of a correlation for each condition is required. The lack of generality and consequent need for experimental information, even for relatively minor changes in the trailing-edge configuration, seems likely to limit the benefits to be obtained from integral methods.

For blunt, sharp, and round trailing-edge flow where the boundary layer is attached to the end of a sharp trailing edge, it seems adequate to represent the effects of the finite trailing-edge thickness by extending the surface streamlines until they intersect in the wake. For the purposes of boundary-layer calculation, the base pressure may be taken as the average of the pressure and suction-side values at the location where the airfoil is truncated. For the calculation procedures that attempt to provide representation of the onset of separation or of the recirculating flow, there is a need to account for the influence of trailing-edge shape: the geometry of the trailing edge has influence upstream of the initial stages of development of the reverse-flow boundary layer and, thus, affects the structure and the size of the back-flow region. The scale of the flow in this region, which includes a second counter-rotating recirculation within the back flow, is small compared to the scale of the boundary layer or outer inviscid flow.

Calculated results confirm the requirements for representation of cross-stream pressure gradients and turbulence normal stresses in the trailing-edge region determined from experiments. Cebeci et al.,<sup>23</sup> found the accuracy of calculations of attached boundary-layer flow to be poorer near the trailing edge, whereas it was acceptable further upstream. Discrepancies were attributable to misrepresentation of normal pressure gradients and turbulence normal stresses upstream of the trailing edge. Chang et al.<sup>50</sup> also calculated turbulent airfoil wakes, and results were acceptable although representation of cross-stream pressure gradients associated with wake curvature was required and appropriate terms were included in the form of a boundary-layer transport equation that was solved. Calculation procedures for attached flows that use boundary-layer approximations but ignore cross-stream pressure gradient do not represent the flow or its development sufficiently accurately, especially for drag, in the region near the trailing edge where the adverse pressure gradient on the surface changes to a favorable pressure gradient in the wake.

The measured importance of cross-stream pressure gradient found in separated flow is also verified in calculations. Mea-



measurements suggest, and calculations confirm, that details of the back flow are of small consequence to the overall flow pattern when compared to the importance of shear layers that separate forward and reversed flow. Transport in the streamwise and cross-stream directions due to turbulence diffusion from this layer can typically exceed 300 and 500%, respectively, of the largest convective transport terms. Characteristics of these shear layers dominate those of the recirculating flow, including its size and, consequently, affect the pressure distribution in the vicinity of the trailing edge. The Navier-Stokes calculations of Reis and Thompson<sup>32</sup> and Adair et al.<sup>10</sup> in separated flows obtained values of pressure gradient normal to the surface that were consistent with experiment: normal pressure gradients in the large recirculation region obtained with the trailing plate at 17.5-deg incidence were calculated to be 11 times greater than those in the flow of Nakayama<sup>15</sup> over the airfoil at 12-deg incidence and 16 times those calculated with the trailing plate at 14-deg incidence and are comparable to measured values. The effect of neglecting the cross-stream pressure gradient terms is also difficult to quantify. A sensitivity analysis to demonstrate the effects of omitting and including the cross-flow momentum term is needed, but requires assurance that the complicating effects of numerical and turbulence assumptions are inconsequential. Some evidence can be gleaned from the surface-pressure calculations of Adair et al.,<sup>10</sup> which included a correction term for the displacement surface curvature and were in poor agreement with measurements in the recirculation region: specifically, the pressure recovery was underpredicted at the upstream end of the recirculation region, and an unphysical favorable pressure gradient occurred at about the center of the backflow over the surface so that the pressure was in good but fortuitous agreement at the trailing edge. The consequences were about a 1% error in lift, but a 30% error in drag obtained from the momentum deficit of the wake.

The largest discrepancies between calculations and measurements are found where large shear stresses occur in the vicinity of recirculation and near wake. Reis and Thompson<sup>32</sup> calculated velocity distributions that qualitatively represented features in the recirculating and wake flow, but values differed from measurements. The drag coefficient obtained by integrating the calculated mean velocity across the wake taking account of static pressure variation, was 20% different from the drag obtained from measurements. Numerical errors contributed to local momentum balances in the region of large shear stress associated with recirculation, and turbulence calculations suggest that turbulence-model assumptions were deficient. It appears that at least the stabilizing and destabilizing effects of streamline curvature, which occur in the attached boundary layer and around the downstream stagnation point of the recirculation bubble, respectively, and also the complex interaction of the suction-side and pressure-side boundary layers with the backflow, are not well represented in the  $k-\epsilon$  turbulence model. Measurements show that the flow patterns near recirculation are strongly dependent on diffusion processes so that their representation is important to the successful calculation of the shear layers that border the forward and reversed flow. The importance of diffusion suggests that diffusion processes need to be better represented in turbulence models and not present in the numerical approximation.

Flows with attached boundary layers at the trailing edge can be represented by simpler turbulence models. Cebeci et al.<sup>23</sup> and Chang et al.<sup>50</sup> preferred a well-found algebraic eddy-viscosity model which allows calculations to be performed about three times faster than with two-equation models and 10 times faster than with Reynolds-stress transport models. Its accuracy was found to be almost within experimental error. Experiments have shown that turbulence normal stresses are important in the trailing-edge region where the turbulence shear stress does not change in proportion to kinetic energy and eddy-viscosity coefficients vary considerably. It is apparent from these results and from the calculations of Adair et al.<sup>10</sup>

and Reis and Thompson<sup>32</sup> that representation of separated trailing-edge flow requires the use of transport equations for streamwise and cross-stream flow, and that these should represent convection, pressure gradient, and turbulence diffusion in both streamwise and cross-stream directions. The solution domain that requires these equations extends from upstream of the trailing edge or separation point to at least two chord lengths downstream of the trailing edge and over at least the wake width.

## V. Conclusions

Our understanding of airfoil and wing flows involves uncertainties including the onset and nature of transition, large vortices and interactions between the flows associated with components such as the fuselage, wing, nacelle, and empennage. Uncertainties also exist due to wind-tunnel characteristics and cannot always be resolved. The following conclusions stem from experiments with simplified configurations and the discussion presented here.

1) Calculated results have uncertainties that are difficult to quantify and increase with angle of attack. It is evident that inviscid flow calculations can provide lift within about 10% for simple airfoils at moderate angles of attack, and that inclusion of viscous effects, through interaction with boundary-layer calculations, can improve this figure even without consideration of the wake.

2) At higher angles of attack where the boundary layer remains attached, it is necessary to include viscous effects and represent the downstream wake. In this way, the maximum in the lift vs angle of attack curve can be represented, although accurate values are likely to require consideration of the cross-stream pressure gradient.

3) Neglect of the effects of the wake and normal pressure gradients has more serious consequences for attached flows on wings at high angle of attack in that they can influence the distributions of pressure and cross-flow velocity and, hence, the accuracy of calculated values of lift, drag, and stability characteristics.

4) In all of the above cases without separation, the turbulence characteristics of the flows can be adequately represented with simple turbulence models.

5) When a large region of suction-side separation exists at the trailing edge, turbulence normal stress becomes important to the momentum balance, but the accuracy of Navier-Stokes and interactive methods are insufficient to resolve the consequences.

6) The influence of trailing-edge thickness of airfoil is small at low angle of attack and can be accommodated in calculation methods. The effect increases with angle of attack and around maximum lift can have an important consequence for lift which cannot be easily accommodated within calculation methods. It can be expected that the influence will be even greater in the calculation of flow around wings.

7) The ability to calculate drag is less satisfactory than for lift and, in most cases, is not adequate for design purposes.

## Acknowledgments

The authors wish to thank SERC (U.K.), NSERC (Canada) and SRA, and colleagues at RAE, SRA and Imperial College.

## References

- <sup>1</sup>Cebeci, T. (ed.), *Numerical and Physical Aspects of Aerodynamic Flows III*, Springer-Verlag, New York, 1986.
- <sup>2</sup>Cebeci, T. (ed.), *Numerical and Physical Aspects of Aerodynamic Flows II*, Springer-Verlag, New York, 1984.
- <sup>3</sup>Holst, T. L., "Viscous Transonic Airfoil Workshop Compendium of Results," AIAA Paper 87-1460, 1987.
- <sup>4</sup>Thompson, B. E. and Whitelaw, J. H., "Characteristics of a Trailing-Edge Flow with Turbulent Boundary-Layer Separation," *Journal of Fluid Mechanics*, Vol. 157, 1985, p. 305.
- <sup>5</sup>Thompson, B. E. and Whitelaw, J. H., "Flow-Around Airfoils with Blunt, Round and Sharp Trailing Edges," *Journal of Aircraft*, Vol. 25, April 1988, pp. 334-342.

- <sup>6</sup>Thompson, B. E. and Whitelaw, J. H., "Flying Hot-Wire Anemometry," *Experiments in Fluids*, Vol. 2, 1984, p. 47.
- <sup>7</sup>Thompson, B. E. and Whitelaw, J. H., "A Turbulent Boundary Layer Approaching Separation," *Waltz-Festschrift Volume*, Springer-Verlag, New York, 1982.
- <sup>8</sup>Thompson, B. E., "The Turbulent Separating Boundary-Layer and Downstream Wake," Ph.D. Thesis, Univ. of London, London, England, 1984.
- <sup>9</sup>Adair, D., Thompson, B. E., Whitelaw, J. H., "Measurements and Calculations of a Separating Boundary Layer and Downstream Wake," *Numerical and Physical Aspects of Aerodynamic Flows III*, edited by T. Cebeci, Springer-Verlag, New York, 1984, pp. 97-111.
- <sup>10</sup>Adair, D., Thompson, B. E., and Whitelaw, J. H., and Williams, B. R., "Comparison of Interactive and Navier-Stokes Calculations of Separating Boundary-Layer Flows," *Numerical and Physical Aspects of Aerodynamic Flows III*, edited by T. Cebeci, Springer-Verlag, New York, 1986.
- <sup>11</sup>Reis, L., "Experimental and Numerical Investigation of the Flow over a Deflected Flap," M.Phil. Thesis, Imperial College, Univ. of London, London, England, 1985.
- <sup>12</sup>Adair, C., "Characteristics of a Trailing Flap Flow With a Small Separation," *Experiments in Fluids*, Vol. 5, 1987, p. 114.
- <sup>13</sup>Acharya, S., Adair, D., and Whitelaw, J. H., "Flow Over a Trailing Flap and in its Asymmetric Wake," *AIAA Journal*, Vol. 25, July 1987, pp. 897-904.
- <sup>14</sup>Nakayama, A., "Characteristics of the Flow Around Conventional and Supercritical Airfoils," *Journal of Fluid Mechanics*, Vol. 160, 1985, pp. 155.
- <sup>15</sup>Nakayama, A., "Measurements of Attached and Separated Turbulent Flows in the Trailing-Edge Region of Airfoils," *Numerical and Physical Aspects of Aerodynamic Flows II*, edited by T. Cebeci, Springer-Verlag, New York, 1986, p. 233.
- <sup>16</sup>Seebohm, T. and Newman, B. G., "A Numerical Method for Calculating Viscous Flow Around Multiple-Section Aerofoils," *Aeronautical Quarterly*, Vol. 26, 1975, p. 176.
- <sup>17</sup>Melnik, R. E., Chow, R., and Mead, H. R., "Theory of Viscous Transonic Flow Over Airfoils at High Reynolds Number," *AIAA Paper 77-0869*, 1977.
- <sup>18</sup>Gilmer, B. R. and Bristow, D. R., "Analysis of Stalled Airfoils Simultaneous Perturbations to Viscous and Inviscid Equations," *AIAA Journal*, Vol. 20, 1982, p. 1160.
- <sup>19</sup>Williams, B. R., "The Prediction of Separated Flow Using a Viscous-Inviscid Interaction Method," *Proceedings of the 14th ICAS Congress*, Toulouse, France, 1984.
- <sup>20</sup>La Balleur, J. C., "Numerical Viscous-Inviscid Interaction in Steady and Unsteady Flows," *Numerical and Physical Aspects of Aerodynamic Flows II*, edited by T. Cebeci, Springer-Verlag, New York, 1984, p. 259.
- <sup>21</sup>Bradshaw, P., Kavenagh, M. A., and Mobbs, D., "Viscous-Inviscid Matching Using Imbedded Navier-Stokes Solutions," *Numerical and Physical Aspects of Aerodynamic Flows II*, edited by T. Cebeci, Springer-Verlag, New York, 1984, p. 125.
- <sup>22</sup>Veldman, A. E. P. and Lindout, J. P. F., "Quasi-Simultaneous Calculations of Strongly Interacting Viscous Flow," *Numerical and Physical Aspects of Aerodynamic Flows III*, edited by T. Cebeci, Springer-Verlag, New York, 1986.
- <sup>23</sup>Cebeci, T., Chang, K. C., Li, C., and Whitelaw, J. H., "Turbulence Models for Wall Boundary-Layers," *AIAA Journal*, Vol. 24, 1986, p. 359.
- <sup>24</sup>Van Dalsem, W. R. and Steger, J. L., "Using the Boundary-Layer Equations in Three-Dimensional Viscous Flow Simulation," *AGARD CP 412*, Paper 24, 1986.
- <sup>25</sup>Briley, W. R. and McDonald, H., "A Survey of Recent Work on Interacted Boundary-Layer Theory for Flow With Separation," *Numerical and Physical Aspects of Aerodynamic Flows II*, edited by T. Cebeci, Springer-Verlag, New York, 1984, p. 141.
- <sup>26</sup>Cebeci, T., Stewartson, K., and Whitelaw, J. H., "Calculation of Two-Dimensional Flow Past Airfoils," *Numerical and Physical Aspects of Aerodynamics Flows II*, edited by T. Cebeci, Springer-Verlag, New York, 1984, p. 1.
- <sup>27</sup>Cebeci, T. and Whitelaw, J. H., "Calculation Methods of Aerodynamic Flows—A Review," *Numerical and Physical Aspects of Aerodynamic Flows III*, edited by T. Cebeci, Springer-Verlag, New York, 1986, p. 1.
- <sup>28</sup>Mehta, U., Chang, K. C., and Cebeci, T., "Relative Advantage of Thin-Layer Navier-Stokes and Interactive Boundary-Layer Procedures," *NASA TM-86778*, 1985.
- <sup>29</sup>Briley, W. R., McDonald, H., and Shamroth, S. J., "A Low Mach Number Euler Formulation and Application to Time-Iterative LBI Schemes," *AIAA Journal*, Vol. 21, 1983, p. 1467.
- <sup>30</sup>Briley, W. R. and McDonald, H., "Solution of the Multidimensional Compressible Navier-Stokes Equations by a Generalized Implicit Method," *Journal of Computational Physics*, Vol. 234, 1977, p. 372.
- <sup>31</sup>Briley, W. R. and McDonald, H., "Three-dimensional Viscous Flows with Large Secondary Velocity," *Journal of Fluid Mechanics*, Vol. 144, 1984, pp. 47-77.
- <sup>32</sup>Reis, L. and Thompson, B. E., "Comparison of Finite Difference Calculations of a Large Region of Recirculating Flow Near an Airfoil Trailing-Edge," *AGARD CP 412*, Paper 19, 1986.
- <sup>33</sup>McGuirk, J. J., Taylor, A. M. K. P., and Whitelaw, J. H., "The Assessment of Numerical Diffusion in Upwind Difference Calculations of Turbulent Recirculating Flow," *Turbulent Shear Flows 2*, Springer-Verlag, New York, 1981, p. 206.
- <sup>34</sup>Bradshaw, P., Cebeci, T., and Whitelaw, J. H., *Engineering Calculation Methods for Turbulent Flow*, Academic Press, London, 1981.
- <sup>35</sup>Shang, J. S., "An Assessment of Numerical Solutions of the Navier-Stokes Equations," *AIAA Paper 85-1549*, 1984.
- <sup>36</sup>MacCormack, R. W., "Current Status of Numerical Solutions of the Navier-Stokes Equations," *AIAA Paper 85-0032*, 1985.
- <sup>37</sup>Shang, J. S. and Hanley, W. L., "Application of Navier-Stokes Equations to Solve Aerodynamic Problems," *AGARD CP 412*, Paper 27, 1986.
- <sup>38</sup>Shamroth, S. J. and Gibeling, H. J., "Navier-Stokes Solution of the Turbulent Flow Field Over Airfoils," *AIAA Journal*, Vol. 18, 1980, p. 1402.
- <sup>39</sup>Sugavanam, A. and Wu, J. C., "Numerical Study of Separated Turbulent Flow Over Airfoils," *AIAA Journal*, Vol. 20, 1982, p. 464.
- <sup>40</sup>Hegna, H. A., "Numerical Solution of Incompressible Turbulent Flow Over Airfoils Near Stall," *AIAA Journal*, Vol. 20, 1982, p. 29.
- <sup>41</sup>Rhie, C. M. and Chow, W. L., "A Numerical Study of the Turbulent Flow Past an Isolated Airfoil with Trailing-Edge Separation," *AIAA Journal*, Vol. 21, 1983, p. 1525.
- <sup>42</sup>Shang, J. S. and Scherr, S. J., "Numerical Simulation of the Flow Field Around a Complete Aircraft," *AGARD CP 412*, Paper 32, 1986.
- <sup>43</sup>Chaderjian, N. M., "Transonic Navier-Stokes Wing Solutions Using a Zonal Approach," *AGARD CP 412*, Paper 30, 1986.
- <sup>44</sup>Raithby, G. D., "Skew-Upwind Differencing Schemes for Problems Involving Fluid Flow," *Computer Methods in Applied Mechanics and Engineering*, Vol. 9, 1976, p. 153.
- <sup>45</sup>Leonard, B. P., "A Stable and Accurate Convective Modeling Procedure Based on Quadratic Upstream Interpolation," *Computer Methods in Applied Mechanics and Engineering*, Vol. 22, 1979.
- <sup>46</sup>Leschziner, M. A., "Practical Evaluation of Three Finite Difference Schemes for the Computation of Steady-State Recirculating Flows," *Computer Methods in Applied Mechanics and Engineering*, Vol. 23, 1980, p. 293.
- <sup>47</sup>Gilmer, B. R., Jasper, D. W., and Bristow, D. R., "Analysis of Stalled Multi-Element Air Foils," *AIAA Paper 84-2196*, 1984.
- <sup>48</sup>Lock, R. C. and Williams, B. R., "Viscous-Inviscid Interactions in External Aerodynamics," *Progress of Aerospace Science*, Vol. 24, 1987, p. 51.
- <sup>49</sup>East, L. F., "A Representation of Second Order Boundary-Layer Effects in the Momentum Integral Equation and in Viscous-Inviscid Interactions," *Royal Astronautical Establishment RAE TP 81002*, 1981.
- <sup>50</sup>Chang, K. C., Bui, M. N., Cebeci, T., and Whitelaw, J. H., "The Calculation of Turbulent Wakes," *AIAA Journal*, Vol. 24, 1986, p. 200.